Turkish Journal of Earth Sciences (Turkish J. Earth Sci.), **Vol. 14**, 2005, pp. 185–207. *Copyright ©TÜBİTAK*

Petrography and Petrology of the Calc-Alkaline Sarıhan Granitoid (NE Turkey): An Example of Magma Mingling and Mixing

ZAFER ASLAN

Karadeniz Teknik Üniversitesi, Gümüşhane Mühendislik Fakültesi, Jeoloji Mühendisliği Bölümü, Bağlarbaşı, TR–29000 Gümüşhane, Turkey (E-mail:aslan@ktu.edu.tr)

Abstract: There are many acidic intrusions of varying age in the northern and southern zones of the eastern Pontides, NE Turkey, and the Sarıhan Granitoid is one of these. The Maastrichtian Sarıhan Granitoid was emplaced into the pre-Permo–Carboniferous Pulur Massif, generally comprising medium-grade metamorphic rocks; the Liassic Hamurkesen Formation, that begins with the Dikmetaş conglomerate and continues upward into volcano-sedimentary rocks; and the Malm–Lower Cretaceous Hozbirikyayla Formation, comprising limestone and sandy limestones. The Sarıhan Granitoid crops out in an area of approximately 40 km^2, has an ellipsoidal shape, and comprises mainly quartz monzodiorite, granodiorite and lesser quartz diorite. The pluton contains volcanic and silicified limestone xenoliths and dioritic mafic microgranular enclaves. The plutonic rocks show medium-grained, poikilitic, monzonitic, anti-rapakivi and sometimes myrmekitic textures, and contain 43–64% plagioclase, 6–18% orthoclase, 10–29% quartz, 5–20% hornblende, 1–85% biotite, 1–6% opaque oxides, accessory amounts of apatite, titanite and zircon, and secondary phases of calcite, chlorite and sericite. Some textures may suggest magma mixing, whereas the presence of mafic microgranular enclaves indicates that magma-mingling processes were operative in the evolution of the pluton. The pluton has 65–67% SiO_2, 1.4–3.1% MgO, 4.1–5.5% Na_2O and <1 K_2O/Na_2O. Generally, the pluton is I-type, metaluminous and has characteristics of cafemic-group granitoids, suggesting a hybrid source derived by mixing of sialic and mantle sources. The pluton has calc-alkaline composition and is characterised by a calc-alkaline granodiorite-series trend. TiO_2, Al_2O_3, FeO, Fe_2O_3, MnO, MgO, CaO, P_2O_5, Ba and Ni decrease whereas Na_2O, K_2O, Rb and Nb increase with increasing SiO_2 content. These geochemical variations indicate the importance of fractional crystallisation, which was mainly controlled by plagioclase and hornblende. However, some irregular variations in major and trace elements may be results of magma mixing. Zn, Rb, Sr, La, Pb, Th and Zr show enrichment whereas Ce, Cr and Ni exhibit depletion compared to continental crust values, resembling those of volcanic-arc granitoids. With regard to discrimination of tectonic setting, the pluton represents pre-plate collision volcanic-arc granitoids. The $^{87}Sr/^{86}Sr$ ratio (0.70504) of the pluton also indicates a hybrid magma which likely was derived by mixing of a mantle source with a crustal component. Field observations suggest a stoping type of ascent and emplacement style.

Key Words: eastern Pontides, Sarıhan Granitoid, mafic microgranular enclaves, magma mixing/mingling, Rb/Sr isotope, petrology, calc-alkaline volcanic-arc granite

Kalk-Alkalin Sarıhan Granitoyidi'nin (KD Türkiye) Petrografisi ve Petrolojisi: Magma Karışımına Bir Örnek

Özet: Doğu Pontidler (KD Türkiye) kuzey ve güney kuşağında değişik yaşlarda pek çok asidik sokulum mevcuttur. Sarıhan Granitoyidi bunlardan biridir. Doğu Pontid güney kuşağında bulunan Maastrihtiyen yaşlı Sarıhan Granitoyidi, genellikle orta dereceli metamorfik kayaçlardan oluşan Permo–Karbonifer öncesi yaşlı Pulur Masifi'ni, Dikmetaş konglomera üyesi ile başlayıp volkano-sedimanter kayaçlarla devam eden Liyas yaşlı Hamurkesen Formasyonu'nu ve kireçtaşı-kumlu kireçtaşından oluşan Malm–Geç Kretase yaşlı Hozbirikyayla Formasyonu'nu keserek yerleşmiştir. Arazi gözlemlerine göre yükselim-yerleşim modeli '*stoping*' tipinde olan ve yaklaşık 40 km^2 bir alanda ellipsoidal şekilde izlenen Sarıhan Granitoyidi genellikle kuvars-monzodiyorit, granodiyorit ve kuvars-diyoritten oluşmaktadır. Sokulum, volkanik ve silisleşmiş kireçtaşı ksenolitleri ile diyoritik mafik mikrogranüler anklavlar içermektedir. Orta taneli, poikilitik, monzonitik, anti-rapakivi ve bazende mirmekitik doku gösteren kalk-alkalin bileşimindeki pluton, %43–64 plajiyoklas, %6–18 ortoklas, %10–29 kuvars, %5–20 hornblend, %1–8 biyotit, %1–6 opak mineral ile apatit, titanit ve zirkon gibi tali mineraller ve kalsit, klorit ve serisit gibi ikincil mineraller içermektedir. Sokulumda tespit edilen bazı dokuların bulunması magma karışmasına (mixing), anklavların bulunması da magma karışmasına (mingling) işaret etmektedir. Sokulum % 65–67 SiO_2, % 1.4–3.1 MgO, % 4.1–5.5 Na_2O ve <1 K_2O/Na_2O değerlerine sahiptir. I tipi ve metalümin özelliğindeki pluton, kafemik grup granitlerin özelliğini olan, sialik ve manto kökenli kaynakların karışımından türeyen melez kaynak özelliği sunmaktadır. Kalk-alkalin bileşimindeki pluton kalk-alkalin granodiyorit serilerin yönelimlerine karşılık gelmektedir. Harker diyagramındaki SiO_2'ye karşı TiO_2, Al_2O_3, FeO, Fe_2O_3, MnO, MgO, CaO, P_2O_5, Ba ve Ni değerleri azalırken Na_2O, K_2O, Rb ve Nb değerlerinin artması, plajiyoklas ve hornblend tarafından kontrol edilen kesri (fraksiyonel) kristallenmeyi işaret etmektedir. Bununla birlikte ana ve iz elementlerdeki düzensiz değişimler magma kirlenmesinden kaynaklanabilir. Kıtasal kabuğa göre normalize edilen iz elementlerden Zn, Rb, Sr, La, Pb, Th ve Zr değerleri zenginleşirken Ce, Cr ve Ni değerlerinde bir azalma söz konusu olup volkanik yay granitlerinin özelliklerini göstermektedir. Tektonik olarak pluton, volkanik yay granitlerinin özelliğini sunmaktadır. $^{87}Sr/^{86}Sr$ oranının 0.70504 olması magma kökenli kaynak ile kabuğun karışımından oluşan melez magma kökenine işaret etmektedir.

Anahtar Sözcükler: Doğu Pontidler, Sarıhan Granitoyidi, mafik mikrogranüler anklav, magma karışımı, Rb/Sr izotop, petroloji, kalk-alkalin volkanik yay graniti

Introduction

Turkey is divided into three major tectonic regions: the Taurides, Anatolides and Pontides (Figure 1; Ketin 1966). The eastern Pontides, rising steeply from the Black Sea coast inland to about 200 km south, form the northern margin of Anatolia. The eastern Pontide terrane is an example of palaeo-island arc generation and long-term crustal evolution from pre-subduction rifting, through arc volcanism and plutonism, to post-subduction alkaline volcanism (e.g., Akın 1978; Şengör & Yılmaz 1981; Akıncı 1984). The eastern Pontides are subdivided into northern and southern zones in northeastern Turkey (Gedikoğlu 1978). These two zones exhibit distinctive features. The northern zone consists of acidic and basic volcanic rocks whereas the southern zone is characterised by sedimentary and metamorphic rocks (Figure 2) (Adamia *et al.* 1977). The rocks of northern zone are younger than those of southern zone (Keskin *et al.* 1989). The volcanic rocks of the eastern Pontides lie unconformably on a heterogeneous Palaeozoic crystalline basement called the Pulur Massif, consisting of metamorphic sequences of varying metamorphic grades, and are cross-cut by granitoids of Permian age (Yılmaz 1972; Çoğulu 1975; Gedikoğlu 1978; Topuz 2000). The Upper Palaeozoic sequence has been studied by several workers (e.g., Ağar 1977; Okay & Şahintürk 1997). Liassic volcanic rocks, tholeiitic in character, mostly crop out in the southern zone, and are composed of basalt with minor andesitic and trachyandesitic lavas (and pyroclastic equivalents). These are overlain conformably

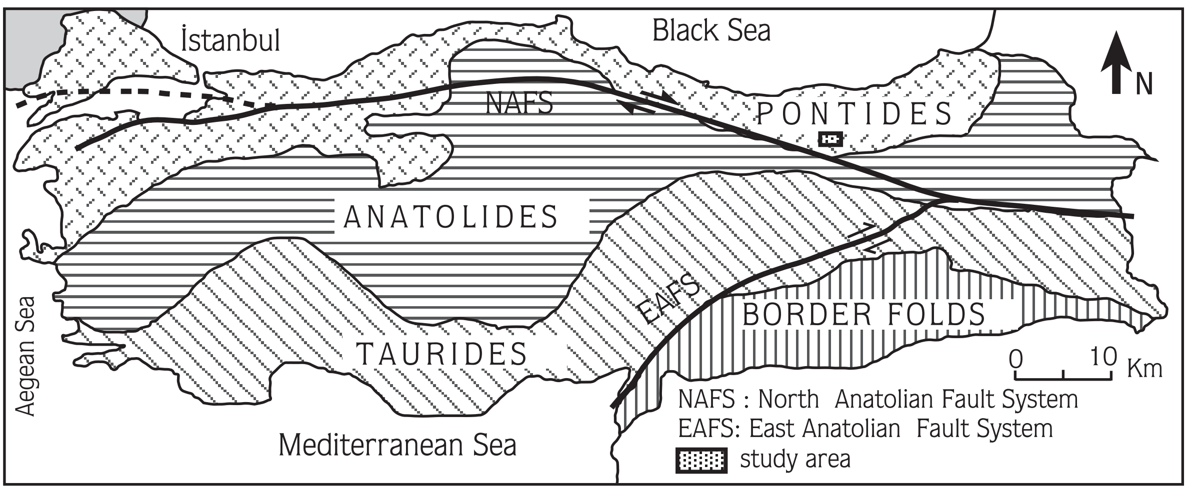

Figure 1. Tectonic map of Turkey (from Ketin 1966).

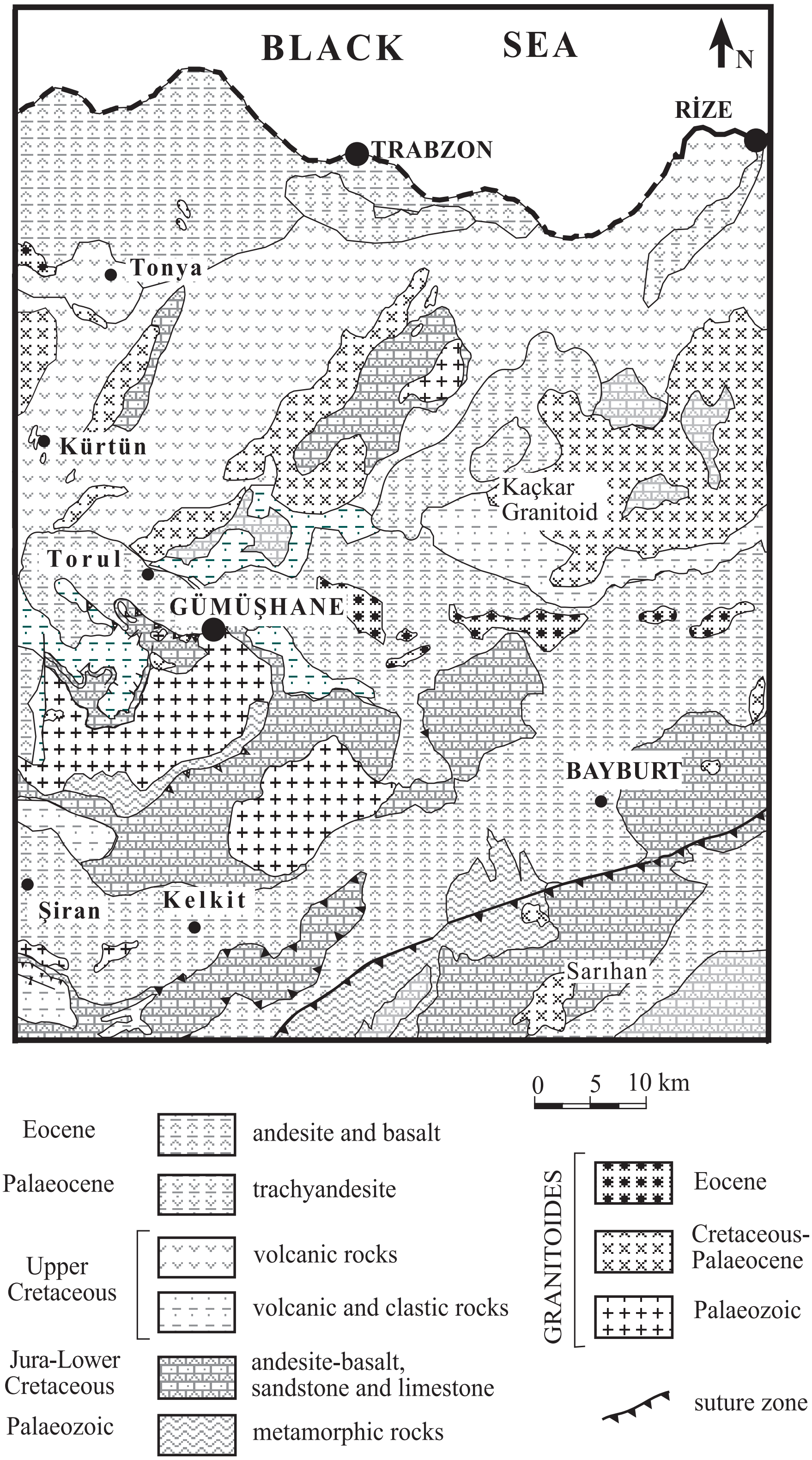

Figure 2. Geological map of the eastern Pontides (from Güven 1993).

by Dogger–Malm–Cretaceous pelagic carbonates. The Upper Cretaceous series unconformably overlie these carbonate rocks, and is dominated by sedimentary rocks in the southern zone and by volcanic rocks in the northern part of the eastern Pontides (Bektaş *et al.* 1987).

The eastern Pontides are also characterised by widespread acidic intrusions of varying age in both the northern and southern zones. These intrusions were emplaced in the Palaeozoic, Cretaceous and Eocene time intervals, and all have the general characteristics of calc-alkaline arc granites (Şen & Kaygusuz 1998; Aslan & Aslaner 1998). In the region, magmas had a range of ages and composition, probably reflecting emplacement into variable geodynamic environments (Çoğulu 1975; Taner 1977; Gedikoğlu 1978; Boztuğ *et al.* 2002, 2003; Moore *et al.* 1980; Van 1990; Okay & Şahintürk 1997; Yılmaz *et al.* 1997; Aslan & Aslaner 1998). Whole-rock compositions range from low-K tholeiitic through calc-alkaline metaluminous granitoids and peraluminous leucogranites to silica-oversaturated alkaline syenites and monzonites (Yılmaz & Boztuğ 1996; Boztuğ 2001; Boztuğ *et al.* 2002, 2003). The geodynamic environments of emplacement include arc-collision, syn-collisional crustal thickening and post-collisional extensional regimes (Yılmaz & Boztuğ 1996; Okay & Şahintürk 1997; Yılmaz *et al.* 1997; Boztuğ *et al.* 2004).

Geological Setting

Since the eastern Pontide region constitutes an old magmatic-arc environment, it is made up of various magmato-tectonic rocks that developed from the Lias through the Eocene. These rocks are generally volcanic and volcanic-related intrusive in nature (Arslan *et al.* 1997).

The study area is located in the southern zone of the eastern Pontides, NE Turkey (Figure 1). The basement in the area is the pre-Permo–Carboniferous Pulur Massif, consisting generally of medium-grade, in some cases low- and high-grade, metamorphic rocks such as greenschist, mica schist, para-amphibole schist, ortho-amphibolite, gneiss, marble and quartzite (Aslan 1998; Okay & Şahintürk 1997). An Upper Palaeozoic sequence has been studied by several workers who have developed conflicting views concerning its stratigraphy and age (e.g., Ağar 1977; Robinson *et al.* 1995; Okay & Şahintürk 1997; Yılmaz *et al.* 1997; Karslı *et al.* 2004). The Middle Carboniferous Saraycık Granodiorite, which has the characteristics of calc-alkaline, I-type, cafemic-group granitoids, cuts the Pulur Massif. Due to this intrusion, epidote hornfels and a skarn zone containing magnetite and hematite formed locally at the contact with country rocks. The Liassic Hamurkesen Formation, which unconformably overlies the massif, begins with the Dikmetaş conglomerate and continues upward with volcano-sedimentary rocks (andesite, basalt, sandstone, limestone, and crystal-vitric tuff), all of which are cut by diabase dykes. The Malm–Lower Cretaceous Hozbirikyayla Formation conformably overlies the Hamurkesen Formation and comprises limestone and sandy limestone. The Hozbirikyayla Formation is conformably overlain by the Otlukbeli mélange, comprising red limestone, pyroclastic rocks, serpentinite, radiolarite, limestone olistoliths and brecciated basalt. The Maastrichtian Sarıhan Granitoid cuts all of these lithologies (Figure 3). Alluvium is the youngest rock unit in the area.

In the region, the first detailed geological study was made by Ağar (1977). According to this study, the age of Sarıhan Granitoid is Palaeozoic and of granodioritic composition. Tanyolu (1988) reported that the Sarıhan intrusion is granodioritic and monzodioritic in composition and Cretaceous in age.

Field Characteristics of the Sarıhan Granitoid

The Sarıhan Granitoid covers an area of approximately 40 km^2 with an ellipsoidal outcrop pattern. The intrusion is made up of quartz monzodiorite (60%), granodiorite (35%) and quartz diorite (5%), and all of which have similar petrographic features. Five- to 10-cm-wide aplites cut across the intrusion. Epidote hornfels and epidotite has developed locally because the Sarıhan Granitoid cut the Hamurkesen Formation at its northwestern border. Marble, recrystallised limestone and a skarn zone have developed at the contact with the Hozbirikyayla Formation, south of Alevi Hill and surrounding Umurlu village to the east of the intrusion, and at Büyükdağ Hill and Sağırınçayır Hill at the southwestern edge of the intrusion. The main ore mineral of the skarn zone is massive, dark magnetite. Additionally, hematite, goethite and malachite are present. The extent of the mineralisation has been determined using the anisotropic

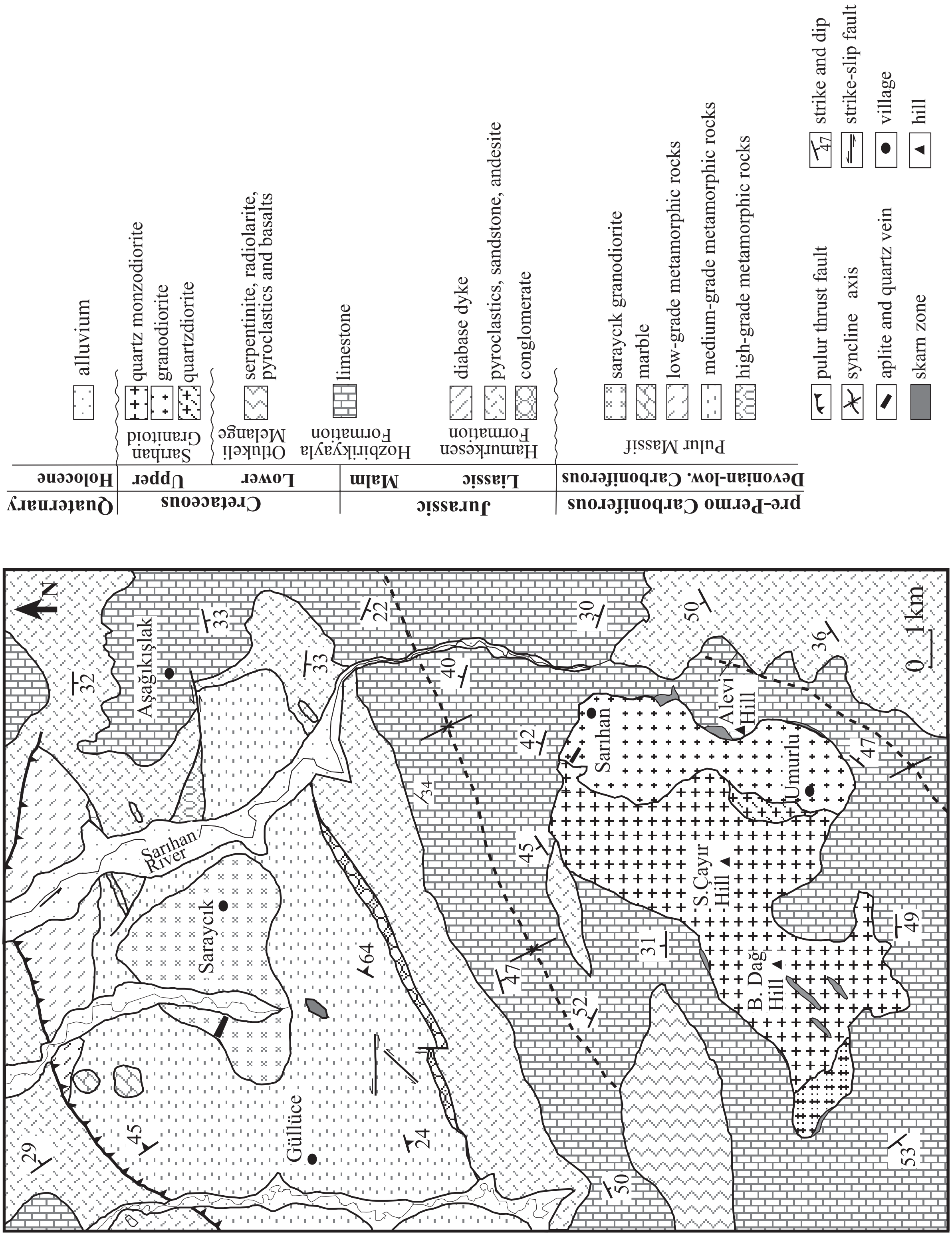

Figure 3. Geological map of the study area (from Aslan 1998).

magnetic susceptibility (AMS) technique. The AMS study suggests that an ore body underlies the contact between the intrusion and limestone, dipping at an angle of 40–60° and reaching a depth of 800 meters (Aslan 1998). In polished sections of the ore, it is observed that the magnetite is altered to martite and muchketovite from the grain margins inward. Furthermore, goethite, lepidocrocite and hematite are also present, as is scarce malachite in oxidation zones within fractures. There is extensive alteration to clay and chlorite in the Umurlu village and Büyükdağ hill areas that is especially concentrated at the border of the intrusion.

The intrusion contains angular volcanic and silicified limestone xenoliths (4–5 cm in diameter) and abundant oval, dioritic mafic microgranular enclaves (MME), medium to dark grey in colour and with diameters of 1–4 cm (Figure 4). Mineralogically, the MME classify as diorites and quartz diorites. The MMEs contain abundant hornblende and some K-feldspar crystals 0.2–0.4 cm in diameter. Xenoliths are characterised by epidotisation at their contacts whereas the MMEs have very sharp contacts without epidotisation. Some joints related to cooling of the pluton are filled by tourmaline crystals.

Figure 4. MME in the Sarıhan Granitoid.

Analytical Methods

Two hundred samples were collected from the studied pluton. Petrographic observations of fifty thin sections were made. The modal mineralogy of selected samples was determined by point counting with a Swift automatic counter fitted to a polarizing microscope. A total of 500 to 650 points were counted in each thin section. Modes were normalized to 100%. Approximately 1 kg samples were collected for whole-rock geochemical analyses. The samples were powdered to smaller than 200 mesh. Major- and trace-element compositions were determined using a RIX 1000 XRF with Rh tube, and mineral identifications were accomplished using a Rigaku D max IIIC XRD with Cu tube an Ni filter at Karadeniz Technical University, Trabzon, Turkey.

Compositions of orthoclase, plagioclase, hornblende and biotite crystals were determined using a CAMECA-SX 50 electron microprobe at Glasgow University (U.K.). Synthetic and naturally occurring oxides were used for calibration in the course of these analyses. About 400 spot analyses were obtained from both rims and cores of each of the four minerals.

8–10 kg samples were collected for whole-rock Rb/Sr isotopic analyses. The samples were powdered, dissolved in HF: NHO_3, and separated using a Rb and Sr standard cation cronomathograph. Compositions were determined in the laboratory of Geospec Consultants Limited (Alberta, Canada) by mass spectrometry using NBS standard reference 987 (0.71024±0.00001).

Petrography

The medium-grained Sarıhan Granitoid is characterised by poikilitic, monzonitic, anti-rapakivi and sometimes myrmekitic textures, and is comprised of 40–65% plagioclase, 10–29% quartz, 6–18% orthoclase, 4–12% hornblende, 1–8% biotite and 1–4% opaque minerals. In addition, important accessory phases apatite, titanite and zircon, and varying amounts of secondary minerals sericite, calcite and chlorite, are present. Plagioclase, the dominant mineral in the pluton, is mainly oligoclase and, in a few cases, andesine (An_{26-38}). The euhedral and subhedral plagioclase may show oscillatory zoning, albite twinning and prismatic-cellular growths (Figure 5a). Myrmekitic texture developed at the contacts of orthoclase and plagioclase crystals. Plagioclase also shows anti-rapakivi texture, mantled by orthoclase (Figure 5b).

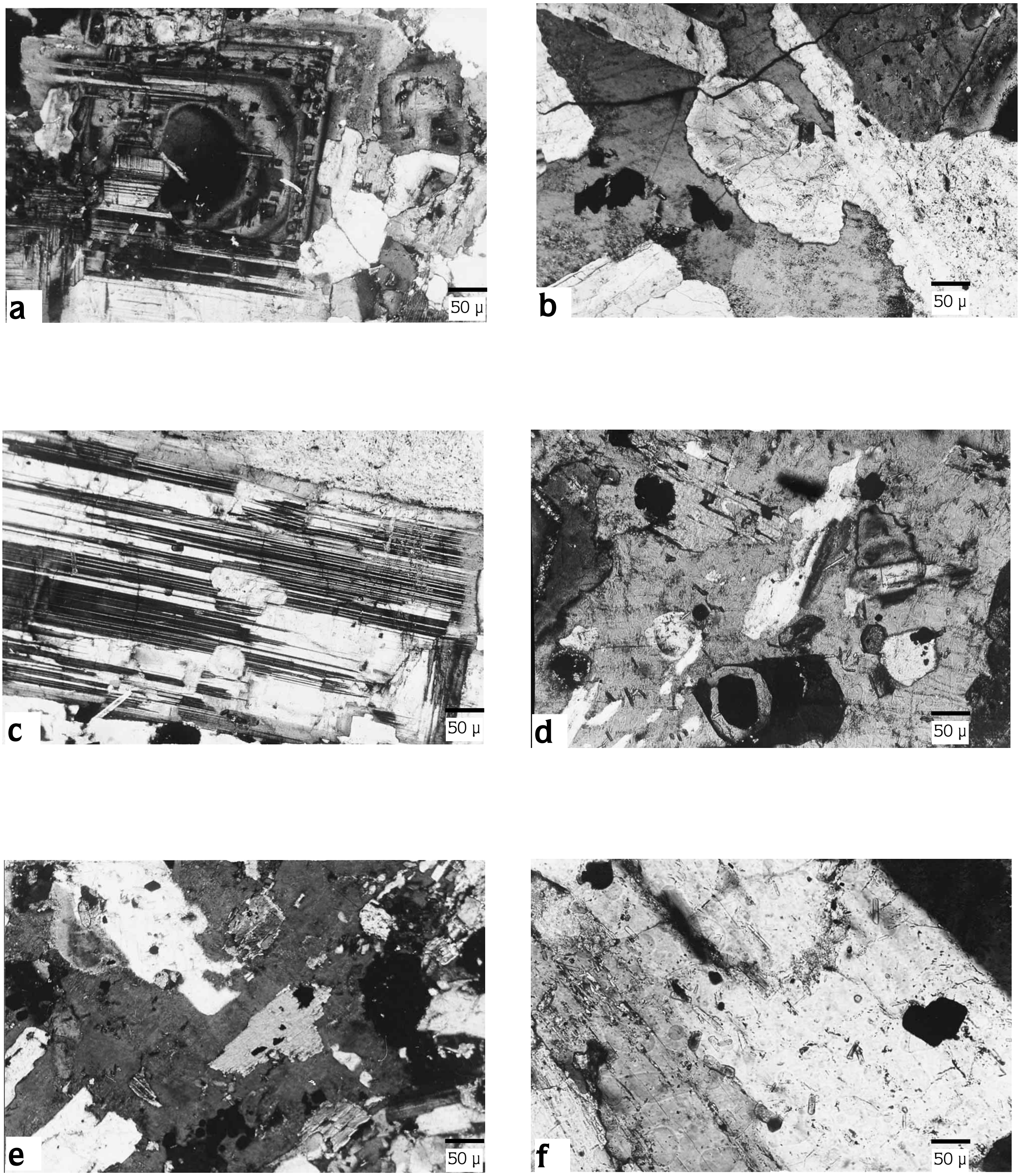

Figure 5. (a) Prismatic-cellular plagioclase; (b) anti-rapakivi texture; (c) small plagioclase inclusions in large plagioclase; (d) poikilitic texture; (e) arrangement of hornblende and biotite inclusions in K-feldspar; (f) acicular apatite crystals. (Pl: plagioclase; Or– orthoclase, Bi– biotite, Hbl– hornblende, Ap– apatite).

In addition, some large plagioclase crystals may contain small plagioclase (Figure 5c), apatite, magnetite and/or hornblende inclusions. Subhedral orthoclase may show poikilitic texture in which abundant quartz, biotite, hornblende, plagioclase and opaque oxides are included (Figure 5d). These inclusion minerals, such as hornblende and biotite grains, are arranged parallel to cleavage in some orthoclase crystals (Figure 5e). The orthoclase may also contain acicular apatite crystals (Figure 5f). Quartz occurs as subhedral to anhedral crystals with irregular cracks and undulatory extinction, and hornblende is present as euhedral to subhedral crystals. Hornblende in the marginal part of the intrusion is fragmented and generally altered to chlorite. It has also been noted that the amount of hornblende decreases from the south to the north side of the intrusion, but that the amount of biotite increases. Biotite characteristically occurs as subhedral crystals, and some biotite is mantled by hornblende at the margins of mafic microgranular enclaves (Aslan 1999). Overall, the ratio of mafic minerals increases from the south to the north side of the intrusion.

Opaque phases, which accompany biotite and hornblende, are mainly magnetite and hematite.

Mineral Chemistry

The results of microprobe analyses of plagioclase, orthoclase, hornblende and biotite are reported in Tables 1 & 2. The composition of orthoclase is An_{0-1} Ab_{12-30} Or_{69-87} and plagioclase is An_{18-37} Ab_{55-79} Or_{22-9} (Figure 6). Plagioclase crystals with oscillatory zoning irregularly range in composition from An_{33} in cores to An_{18} at rims (Aslan 1999). These irregular compositional changes may indicate magma mixing, unstable crystallization, or both (cf. Stamatelopoulou-Seymour *et al.* 1990; Shelley 1993). The change in the %An profile of the oscillatory zoning in the plagioclase may have resulted from magma mixing and unstable crystallization processes. The composition of hornblende in these rocks varies from edenite, through magnesio-hornblende to actinolitic hornblende (Figure 7a, b; Aslan 1999). Magnesio-hornblende and actinolitic hornblende occurs at the margins whereas edenite occurs in the centre of the intrusions. Geobarometric calculations (cf. Hammarstrom & Zen 1986; Hollister *et al.* 1987) on the hornblendes yield 0.40–0.80 kbar from the margin, 1.7–2.6 kbar from the centre of the granitoid. Thus, on the basis of these geobarometric data, the depth of the intrusion was 2–10 km, corresponding to epizonal granitoids. Biotite composition ranges from 29–30% phlogopite to 60–71% annite component (Figure 8).

Features of the Magma Mixing and Mingling

Enclaves are important features of granitic magmas and their origin constitutes a complex problem. Field evidence for magma mingling and textural-geochemical evidence for magma mixing have been determined for the Sarıhan Granitoid. It contains volcanic xenoliths and mafic microgranular enclaves (MME). The presence of MME and some microscopic textures in the rock may indicate magma mixing and mingling processes (cf. Hibbard 1991; Pitcher 1993; Yılmaz & Boztuğ 1994). As a result of heterogeneous mixing of two magmas, mafic magmatic enclaves developed with microgranular texture (magma mingling), and some textural features developed due to homogeneous mixing of magmas (cf. Barbarin & Didier 1992). Textural features described by Fernandez & Barbarin (1991) are observed in the studied intrusion. These features include anti-rapakivi texture, poikilitic K-feldspar, alignment of hornblende and biotite inclusions in K-feldspar, small plagioclase inclusions in larger plagioclase crystals, acicular apatite in plagioclase, and prismatic-cellular plagioclase growths.

In addition, biotite is generally mantled by hornblende at the contact of MME with the host granitoid (Figure 9a). This feature is also one of the textural features that indicates mixing of mafic and felsic magma and probably resulted from an increase of temperature in a solidifying hybrid magma as shown in Figure 9b. When mafic magma is in the melting phase, biotite crystals are present within the felsic magma. When two magmas are mixed, hornblende occurrences are initiated by taking previously existing biotite as cores for crystallisation. Thus, biotite crystals mantled by hornblende appear within the hybrid system. When the hybrid system reaches equilibrium conditions, euhedral hornblende begins to form (cf. Hibbard 1991).

The presence of K-feldspar megacrysts in the MME may imply that they had a similar origin (cf. Vernon 1991), because K-feldspar megacryst-bearing MME are common in K-feldspar megacrystic granites. K-feldspar forms in the early stages of crystallisation; moreover, the

Table 1. Mineral chemistry of orthoclase and plagioclase (in terms of wt % and cations).

Sam. No	S5-f (r)	S5-f (c)	S6-f (c)	S1plj (c)	S3plj (r)	S5plj (c)	S6plj (r)	S7plj (r)	S7plj (c)	S7plj (c)	S8plj (r-c)	S8plj (c)
SiO_2	63.67	63.67	63.84	58.63	61.76	58.50	61.88	60.02	57.81	62.02	58.42	59.27
TiO_2	0.00	0.00	0.00	0.11	0.00	0.00	0.00	0.01	0.11	0.07	0.02	0.00
Al_2O_3	18.63	18.06	18.50	24.72	22.92	24.28	23.09	23.47	24.54	21.96	25.41	24.99
FeO	0.19	0.14	0.00	0.23	0.24	0.24	0.28	0.12	0.21	0.21	0.27	0.26
MnO	0.03	0.00	0.00	0.03	0.00	0.00	0.00	0.00	0.00	0.00	0.01	0.04
MgO	0.00	0.00	0.02	0.00	0.00	0.00	0.01	0.00	0.00	0.00	0.00	0.00
CaO	0.18	0.17	0.08	6.38	4.71	7.22	6.10	5.34	7.00	4.42	7.05	6.55
Na_2O	2.92	2.86	3.59	8.91	9.96	8.64	9.38	10.02	8.36	10.34	8.56	8.97
K_2O	13.93	13.46	12.53	0.29	0.53	0.28	0.25	0.21	0.32	0.35	0.50	0.54
Total	99.30	98.37	98.57	99.30	100.12	99.15	100.99	99.19	98.36	99.36	100.25	100.62
Si	2.99	2.98	2.97	2.63	2.76	2.63	2.99	2.71	2.64	2.79	2.62	2.65
Ti	0.00	0.00	0.00	0.00	0.00	0.00	0.00	0.00	0.00	0.00	0.00	0.00
Al	0.98	1.00	1.01	1.33	1.21	1.30	1.00	1.25	1.32	1.16	1.34	1.32
Mg	0.00	0.00	0.00	0.00	0.00	0.00	0.00	0.00	0.00	0.00	0.00	0.00
Ca	0.01	0.01	0.00	0.31	0.23	0.35	0.01	0.26	0.34	0.21	0.34	0.31
Mn	0.00	0.00	0.00	0.00	0.00	0.00	0.00	0.00	0.00	0.00	0.00	0.00
Fe	0.01	0.01	0.00	0.01	0.01	0.01	0.00	0.00	0.01	0.01	0.01	0.01
Na	0.27	0.26	0.32	0.79	0.82	0.76	0.13	0.88	0.74	0.90	0.75	0.78
K	0.76	0.80	0.74	0.02	0.03	0.02	0.91	0.01	0.02	0.02	0.03	0.03
Ab	26.07	24.20	30.25	70.54	77.16	67.46	12.02	76.42	67.23	72.76	66.97	69.29
Or	73.06	75.02	69.40	1.53	2.70	1.42	87.50	1.08	1.68	1.87	2.58	2.72
An	0.87	0.78	0.35	27.93	20.15	31.12	0.48	22.51	31.09	25.36	30.45	27.99

- S5, S6-f: orthoclase; S1, S3, S5, S6, S7, S8-plj: plagioclase.
- r: rim of mineral; c: center of mineral; r-c: between rim and center.
- Cations are calculated on the basis of 8 oxygens.

mechanical transfer of K-feldspar megacrysts from a more felsic magma into mafic magma has been suggested as a likely process. Furthermore, irregular changes in the compositions of some plagioclases may indicate magma mixing. This magmatic event is also consistent with the geochemical and Rb-Sr isotopic data.

Geochemisty

Whole-rock Geochemistry

Nineteen samples from the Sarıhan Granitoid were analysed for major and trace elements. These analyses and the CIPW normative mineralogy of the Sarıhan

Table 2. Mineral chemistry of hornblende and biotite (in terms of wt % and cations).

Smp. No	S1 (c)	S1 (r)	S3 (c)	S5 (r)	S5 (c)	S5 (r)	S6 (c)	S7 (c)	S7 (r)	S10 bi-r	S13 bi-c	S18 bi-r
SiO_2	49.20	49.81	47.67	46.48	46.20	46.09	46.58	48.28	47.20	37.80	35.93	37.79
TiO_2	0.87	0.91	1.20	1.40	1.33	1.11	1.27	0.83	1.10	4.97	3.98	4.53
Al_2O_3	4.49	4.65	5.41	6.97	6.52	6.68	6.41	5.11	5.83	12.89	13.53	12.41
Cr_2O_3	0.00	0.04	0.01	0.00	0.04	0.00	0.00	0.00	0.08	0.00	0.00	0.00
FeO	10.99	10.98	10.51	11.45	11.57	11.95	10.34	8.68	8.73	11.17	13.02	13.62
MnO	0.37	0.48	0.36	0.44	0.33	0.61	0.41	0.42	0.29	0.13	0.17	0.19
MgO	15.87	15.33	17.14	14.63	14.97	14.99	15.03	16.36	16.03	15.65	15.93	14.39
CaO	11.98	11.96	11.53	11.87	11.79	11.85	11.19	11.27	10.97	0.33	0.15	0.18
Na_2O	1.34	1.23	1.53	1.78	1.87	1.83	1.76	1.70	1.87	0.27	0.12	0.24
K_2O	0.60	0.55	0.48	0.68	0.64	0.61	0.65	0.39	0.54	9.41	7.98	9.99
H_2O	1.58	1.76	1.84	1.87	1.85	1.82	1.72	1.89	1.88	3.37	3.60	3.61
F	0.91	0.58	0.39	0.30	0.31	0.39	0.55	0.21	0.21	1.23	0.56	0.66
Total	98.20	98.03	98.08	97.87	97.28	97.91	95.92	95.11	94.72	97.20	94.96	97.31
Si	7.29	7.34	7.05	6.94	6.94	6.91	7.05	7.27	7.15	5.73	5.57	5.78
Ti	0.10	0.10	0.13	0.16	0.15	0.13	0.14	0.09	0.13	0.57	0.46	0.52
$Al^{[4]}$	0.71	0.68	0.94	1.06	1.06	1.11	0.95	0.78	0.90	2.02	2.18	1.97
$Al^{[6]}$	0.07	0.13	0.00	0.17	0.09	0.07	0.20	0.12	0.14	0.39	0.41	0.37
Cr	0.00	0.00	0.00	0.00	0.00	0.00	0.00	0.00	0.01	0.00	0.00	0.00
Mg	3.50	3.37	3.78	3.26	3.35	3.35	3.39	3.67	3.62	3.53	3.68	3.28
Ca	1.90	1.89	1.83	1.90	1.90	1.90	1.82	1.82	1.78	0.05	0.03	0.03
Mn	0.05	0.06	0.05	0.06	0.04	0.08	0.05	0.05	0.04	0.02	0.02	0.02
Fe^{+2}	1.36	1.22	1.05	1.43	1.45	1.35	1.31	0.80	0.48	1.48	1.76	1.82
Fe^{+3}	0.00	0.13	0.24	0.00	0.00	0.15	0.00	0.29	0.62	0.00	0.00	0.00
Na	0.38	0.35	0.44	0.52	0.54	0.53	0.52	0.48	0.55	0.08	0.04	0.07
K	0.11	0.10	0.09	0.13	0.12	0.12	0.13	0.07	0.10	1.82	1.58	1.89
P1(kb)	-	-	0.81	2.27	1.86	2.02	1.81	0.66	1.31	-	-	-
P2(kb)	-	-	0.54	2.18	1.73	1.90	1.67	0.37	1.11	-	-	-

- S1: actinolitic hbl; S3, S5, S6: edenite; S7: magnesio-hbl; S10, S13, S18- biotite. r: rim of mineral, c: center of mineral.

- P1 = 5.03*Al^t – 3.92 kb (Hammarstrom and Zen, 1986); P2 = 5.64*Al^t – 4.76 kb (Hollister *et al.* 1987)

- Cations are calculated on the basis of 24 oxygens.

Granitiod are given in Table 3. The intrusion has 65–67% SiO_2, 1.4–3.1% MgO, 4.1–5.1% Na_2O, 3.1–4.8% CaO and <1 K_2O/Na_2O. The Sarıhan Granitoid geochemically consists of quartz diorite, tonalite and granodiorite, and has a calc-alkaline granodiorite-series trend (cf. Lameyre & Bonin 1991) (Figure 10). When the intrusion is classified chemically using the AFM ternary diagram (Irvine & Baragar 1971), the rocks of the Sarıhan Granitoid plot in the calc-alkaline field (Figure 11). The molecular A/CNK ratios of the samples are in the range 0.80–0.91; these values show that the Sarıhan Granitoid is metaluminous in character and of I-type (Figure 12). Moreover, the intrusion shows a cafemic-group granitoid trend in the A-B discrimination diagram of Debon & Le

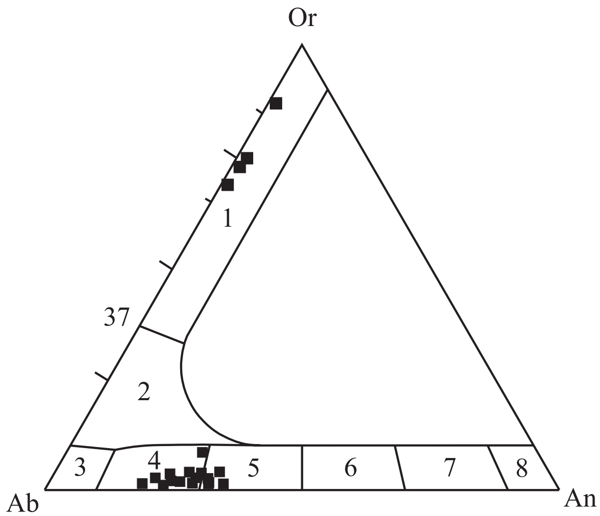

Figure 6. Ab-Or-An triangular diagram of the feldspars. (1) sanidine; (2) anorthoclase; (3) albite; (4) oligoclase; (5) andesine; (6) labradorite; (7) bytownite; (8) anorthite.

Fort (1982) (Figure 13). Cafemic groups are commonly driven by mixing of sialic and mantle-sourced materials of a hybrid origin, wherein mantle-sourced materials contribute more. TiO_2, Al_2O_3, FeO_t, MnO, MgO, CaO, P_2O_5, Ba and Ni decrease whereas Na_2O, K_2O, Rb and Nb increase with increasing SiO_2 content (Figures 14 & 15). These geochemical variations indicate the importance of fractional crystallisation, which was mainly controlled by plagioclase and hornblende phases (Figure 16a-c) (Beckinsale 1979; Atherton & Sanderson 1985; Bussel 1988). However, some irregular variations in major and trace elements may have resulted from magma mixing. Zn, Rb, Sr, La, Pb, Th and Zr show enrichment whereas Ce, Cr and Ni exhibit depletion relative to continental crust values, resembling those of volcanic-arc granitoids (Clarke 1992). Intrusive rock samples from the pluton were normalised to continental crust (Taylor & McLennan 1985) (Figure 17). As it can be seen in that figure, Th, Pb, La, Ba, Zr, Sr, Rb and Zn are enriched; conversely, Cr and Ni are depleted. Nevertheless, Cu, Y, Nb and Ce contents are quite similar to the composition of the continental crust. The emerging trend resembles examples given by Pearce *et al.* (1984), indicating a post-collisional geodynamic evolution.

According to the tectonic discrimination diagram of Batchelar & Bowden (1985), the intrusion is made up of pre-plate collision and post-collisional granitoids (Figure 18). Also, when plotted on the tectonic discrimination diagram of Pearce *et al.* (1984), rocks of the pluton fall into the field for volcanic-arc granitoids (VAG) field in the Rb versus Y+Nb diagram (Figure 19). Most plot in the

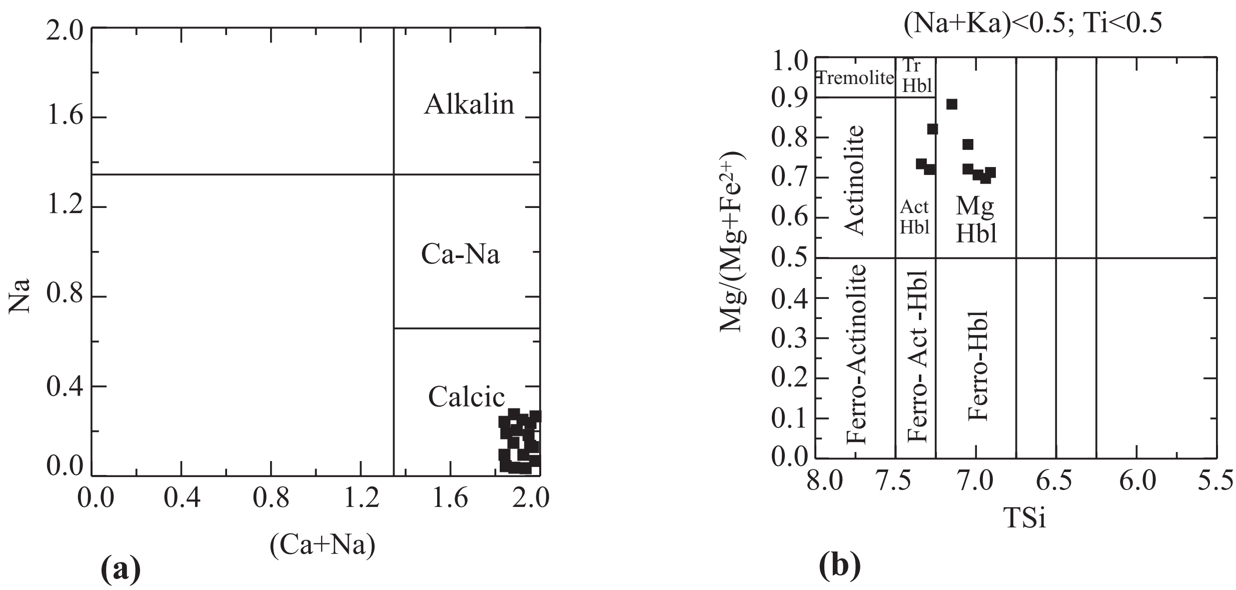

Figure 7. (a) Na – (Ca+Na) diagram; (b) Mg/(Mg+Fe^{2+}) & TSi diagram (after Leake 1978).

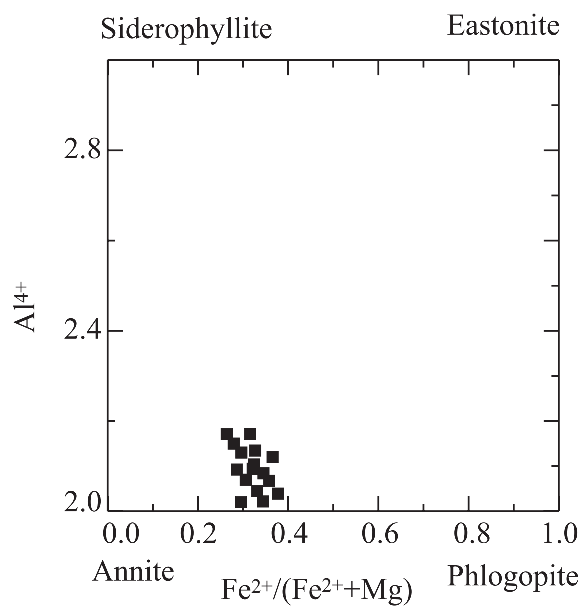

Figure 8. Biotite diagram (after Leake & Said 1994).

upper part of the VAG field, in keeping with the continental setting (Förster *et al.* 1997).

The general geochemical features of the MME are quite similar to the host granitoid. However, the MME are more basic than the granitoid, indicating a magmatic origin for these enclaves (cf. Vernon 1984) or they could also be be stoped, partially re-equilibrated blocks.

Isotope Geology

Rb-Sr whole-rock isotopic studies were made on three selected samples. The samples have Sr contents of 877–909 ppm, and Rb contents of 72–84 ppm; their $^{87}Sr/^{86}Sr$ = 0.70502–0.70507(±0.00001) and $^{87}Rb/^{86}Sr$ = 0.2274–0.2746 (±0.00001). Based on these isotopic data, the initial Sr-isotopic ratio is $(^{87}Sr/^{86}Sr)_i$ = 0.70481 and, in light of this ratio, the age of the intrusion was calculated as 66.634±2 Ma. The high Sr-isotopic value is characteristic of crustal involvement whereas the initial value reflects a mantle origin (Faure 1986) (Figure 20). Furthermore, the $(^{87}Sr/^{86}Sr)i$ value is also representative of I-type granitic rocks. Consequently, these obtained isotopic data suggest a hybrid source for the petrogenesis of the Maastrichtian Sarıhan Granitoid. It is likely that a parental magma derived from an upper-mantle source mixed with crustal material, as borne out by the petrographic and general geochemical data.

Conclusions

In the eastern Pontides, the extent of Cretaceous volcanoes was controlled by NE–SW- and NW–SE-trending principal tectonic features (Bektaş *et al.* 1984), and Upper Cretaceous plutons generally intruded limestones. A large number of granitoid intrusions aged 95 to 65 Ma (Taner 1977) were associated with the Cretaceous volcanism. The Sarıhan Granitoid is an example of the volcanic-arc granitoids that occur in the eastern Pontides, NE Turkey. The granitoid intruded the Malm–Lower Cretaceous Hozbirikyayla Limestone in the southern zone of the eastern Pontides. Field and petrographic characteristics indicate that the granitoid shows characteristics of mafic and felsic magma interaction, including the presence of MME, anti-rapakivi texture, poikilitic texture, alignment of hornblende and biotite inclusions in K-feldspar, small plagioclase inclusions in larger plagioclases, acicular apatite in plagioclase, prismatic-cellular plagioclase growths and mantling of biotite by hornblende. The pluton has the general features of I-type, calc-alkaline, metaluminous and cafemic-group granitoid series.

The granitoid has A/CNK<1.1, $FeO_t/(FeO_t+MgO)$ <0.8 and a $^{87}Sr/^{86}Sr$ initial ratio of 0.705 which are characteristic of hybrid continental-arc granitoids (e.g., Barbarin 1990). All of these data indicate significant magma mixing and mingling processes during the evolutionary history of the pluton.

The Rb-Sr age of the intrusion was reported as 66 Ma by Aslan (1998). The magma source of this pluton may have been generated as result of partial melting of the mantle during the southward-dipping period of the crust of Palaeotethys in Cretaceous time (Bektaş *et al.* 1984). Which resulted in profound crustal thickening. These mantle-derived melts mixed with crustal anatectic melts to form a hybrid magma. In the Maastrichtian, the hybrid magma ascended and was emplaced via stoping into the Malm–Lower Cretaceous limestones.

Acknowledgements

This study was funded by Karadeniz Technical University, Research Fund Project No: 94.112.005.1. The author thanks Prof. Dr Mustafa Aslaner and Assoc. Prof. Mehmet Arslan for constructive comments on and help with the manuscript.

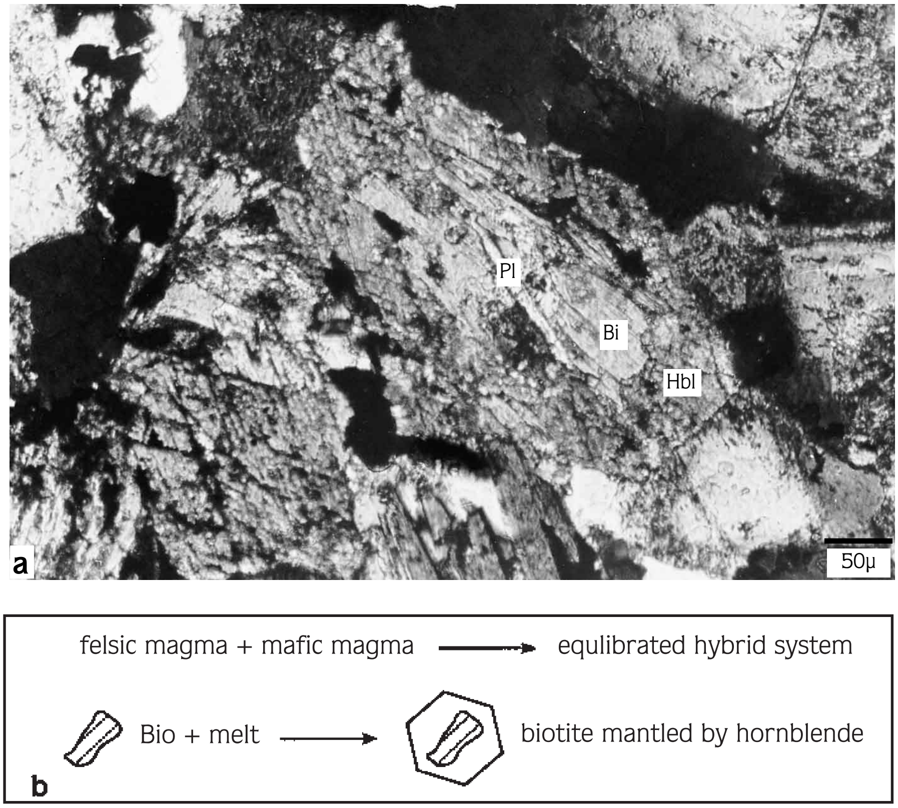

Figure 9. (a) Photomicrograph of biotite mantled by hornblende (Pl– plagioclase; Bi– biotite; Hbl– hornblende); (b) schematic description showing of simple equilibrated hybrid system.

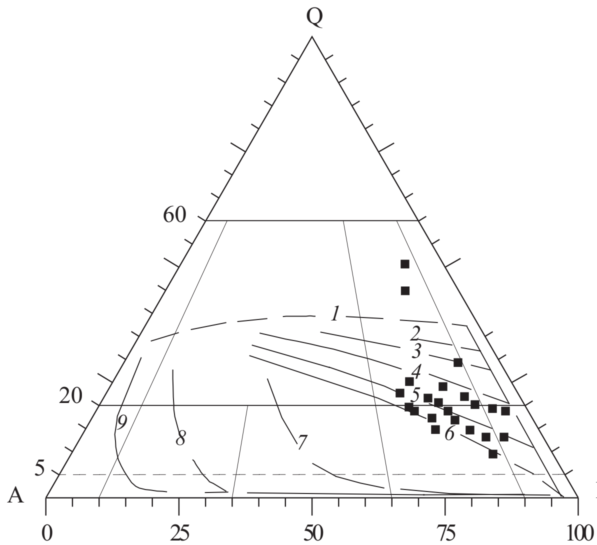

Figure 10. Main trends of some plutonic-type series based on QAP modal compositions (after Lameyre & Bonin 1991). (1) tholeiitic series, (2) calc-alkaline-trondhjemitic series, (3–6) various calc-alkaline-granodiorite series, (7) monzonitic series, (8–9) various alkaline series.

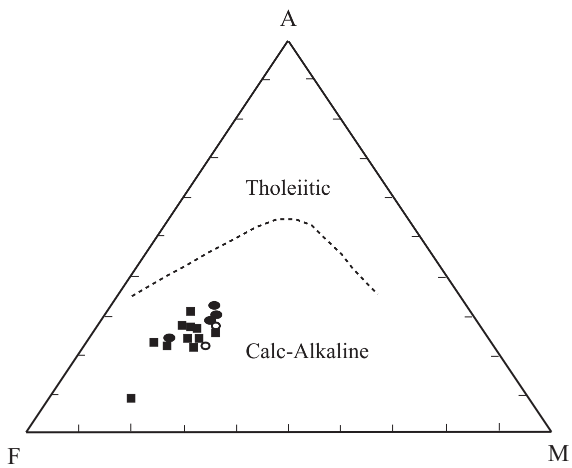

Figure 11. AFM triangular diagram (after Irvine & Baragar 1971). Filled square– granodiorite, filled circle– Q-monzodiorite; open circle – Q-diorite.

Table 3. Whole-rock geochemical data and normative mineralogy for samples from the Sarıhan Granitoid.

	6	7	28	28	32	193	198	201	202	264	S6	S7	226	227	254	282	2	S2	S4
SiO_2	66.73	66.34	68.3	65.65	74.87	67.40	65.58	66.20	66.59	67.09	67.19	66.81	65.07	65.47	65.05	66.04	65.02	67.2	66.02
TiO_2	0.48	0.48	0.33	0.52	0.09	0.42	0.50	0.51	0.51	0.48	0.48	0.48	0.58	0.55	0.55	0.49	0.58	0.46	0.52
Al_2O_3	15.39	15.44	15.45	15.47	13.39	15.38	15.44	15.10	15.23	15.28	15.13	15.35	15.10	15.16	15.25	15.34	15.24	15.20	15.32
Fe_2O_3	1.62	1.68	0.46	1.79	0.28	1.36	1.48	2.02	1.40	1.35	1.44	1.51	2.10	2.02	2.05	1.51	2.05	1.22	1.68
FeO	1.85	1.91	0.52	2.03	0.32	1.55	2.02	2.11	1.39	1.47	1.55	1.64	2.30	2.20	2.23	1.73	2.34	1.43	2.04
MnO	0.05	0.07	0.03	0.06	0.02	0.04	0.06	0.06	0.04	0.05	0.05	0.06	0.06	0.06	0.05	0.03	0.06	0.04	0.06
MgO	2.08	2.39	1.51	2.32	0.28	1.53	3.01	2.20	1.48	2.37	2.39	3.04	2.69	2.83	2.98	1.95	2.97	3.01	3.01
CaO	4.09	4.07	4.11	4.56	0.86	3.90	3.45	3.59	3.48	4.17	4.16	4.35	4.56	4.61	4.62	3.08	4.01	3.55	4.39
Na_2O	4.30	4.37	4.55	4.51	3.09	4.84	5.09	4.42	4.57	4.20	4.27	4.10	4.36	4.24	4.36	5.15	4.33	4.35	4.21
K_2O	2.50	2.16	2.41	2.16	5.18	2.68	2.99	2.43	2.66	2.20	2.39	2.19	2.11	2.18	2.22	2.46	2.19	2.48	2.34
P_2O_5	2.28	0.30	0.28	0.34	0.03	0.23	0.32	0.31	0.33	0.33	0.31	0.34	0.35	0.32	0.33	0.33	0.39	0.34	0.33
LOI	1.45	1.66	1.96	1.06	1.12	1.37	1.75	2.09	1.50	1.64	1.38	1.56	1.74	1.37	1.09	1.51	1.58	1.71	1.41
Total	100.8	100.8	99.93	100.5	99.53	101.2	101.7	101.1	99.18	100.6	100.7	101.3	100.9	101.0	100.8	99.62	100.7	100.8	101.3
Rb	106	122	141	106	142	120	126	107	106	120	114	99	81	80	91	111	94	103	97
Sr	908	946	1135	1099	210	891	805	870	1104	977	947	1042	1063	1047	922	1017	969	1017	976
Zr	195	208	242	214	91	204	196	196	234	200	208	199	203	205	189	199	214	206	200
Y	14	18	19	17	8	15	18	14	16	18	16	17	16	15	14	18	19	17	16
La	166	60	85	154	26	91	73	125	54	59	-	-	75	-	67	148	111	-	-
Ba	791	784	726	744	418	723	736	933	841	780	859	735	694	764	769	706	795	791	751
Ce	12	-	-	-	120	-	-	-	-	7	35	30	-	20	-	-	-	53	25
Nb	12	18	20	17	6	16	14	16	19	14	19	15	15	13	13	14	15	17	15
Th	11	22	14	15	14	15	18	15	19	15	28	33	14	13	14	10	17	32	23
Pb	66	357	100	46	157	253	2067	1908	28	84	251	53	507	239	3371	483	1288	437	340
Q	20.6	18.5	22	17.8	36.7	20.6	14.5	19.1	18.9	19.3	20.04	19.2	18.2	18.7	15.8	17.2	15.7	18.5	17.9
Or	15.2	16.2	15.3	13.8	30.4	15.7	17.5	16	16.8	15.8	17	14.6	12.4	13.4	14.2	16.2	14	15.7	14.9
An	14.6	14.5	12.6	15	4.07	12.3	10.9	13.2	12.2	14.3	14.3	16.3	15.7	15.4	14.4	10.9	15.1	13.5	16.1
Ab	38	38.6	41	40.6	26.1	40.9	43	39	40.3	38	36.1	36.3	37.7	36.6	40.2	44.3	39.9	39.3	37.2
Di	3.06	2.95	4.61	4.32	-	4.43	4.01	3.28	3.09	3.75	3.37	4.4	5.26	5.48	5.83	1.75	4.9	2.69	3.58
Hy	5.18	6.51	1.7	5.22	0.94	2.8	7.12	5.85	4.21	5.65	5.6	6.96	6.12	6.2	6.42	5.3	6.92	7.46	7.43
Mt	2.5	2.44	0.67	2.6	0.41	1.98	2.59	3.08	2.03	2.25	2.24	2.48	3.2	2.93	2.98	2.34	3.12	2.21	2.73
Il	0.91	0.91	0.63	0.99	0.17	0.8	0.95	0.97	0.97	0.91	0.91	0.91	1.1	1.05	1.05	0.93	1.1	0.88	0.99
Mg#	54.4	64.1	83.3	54.3	60.9	47.1	54.3	54.3	47.1	64.1	64.1	54.3	54.3	54.3	54.3	47.1	54.3	64.1	54.3
A/CNK	0.88	0.88	0.85	0.85	1.09	0.86	0.86	0.87	0.88	0.86	0.87	0.85	083	0.82	0.82	0.91	0.83	0.88	0.87

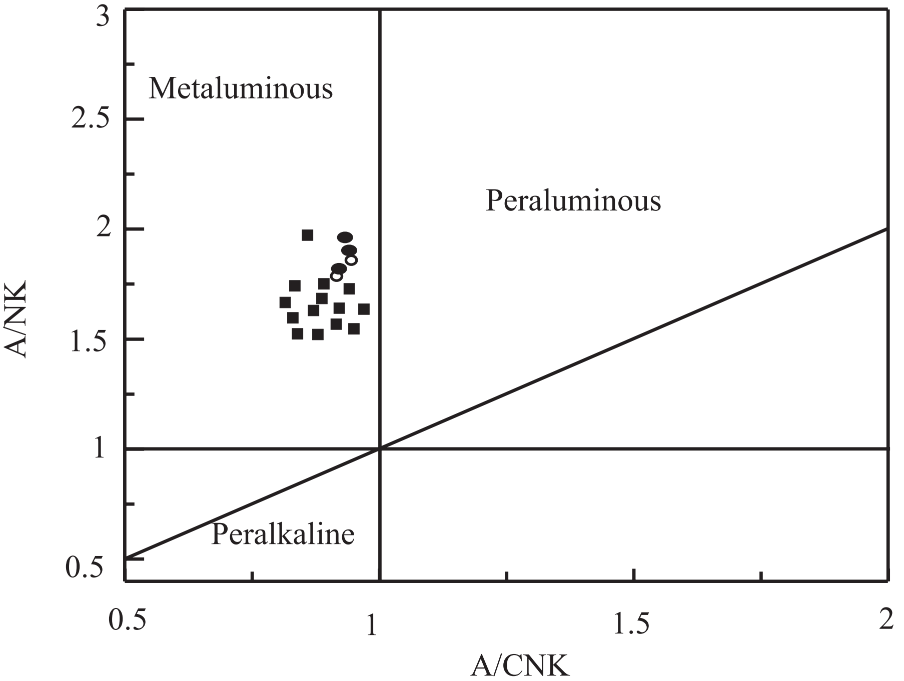

Figure 12. A/NK – A/CNK geochemical discrimination diagram (after Maniar & Piccoli 1989). Filled square– granodiorite, filled circle– Q-monzodiorite; open circle – Q-diorite.

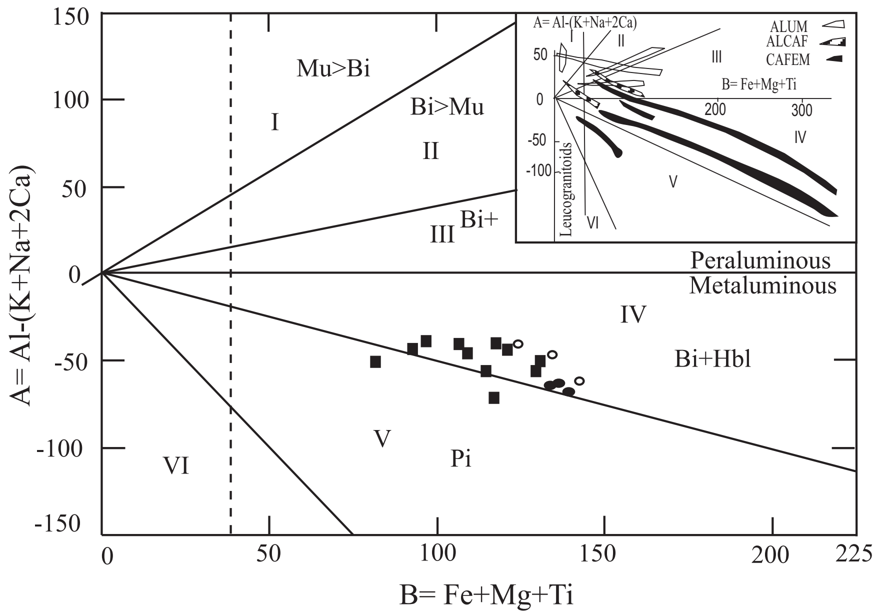

Figure 13. Chemical trends presenting the main magma associations of the plutonic phases in the A-B characteristic-minerals diagram (after Debon & Le Fort 1982). Filled square– granodiorite, filled circle– Q-monzodiorite; open circle – Q-diorite.

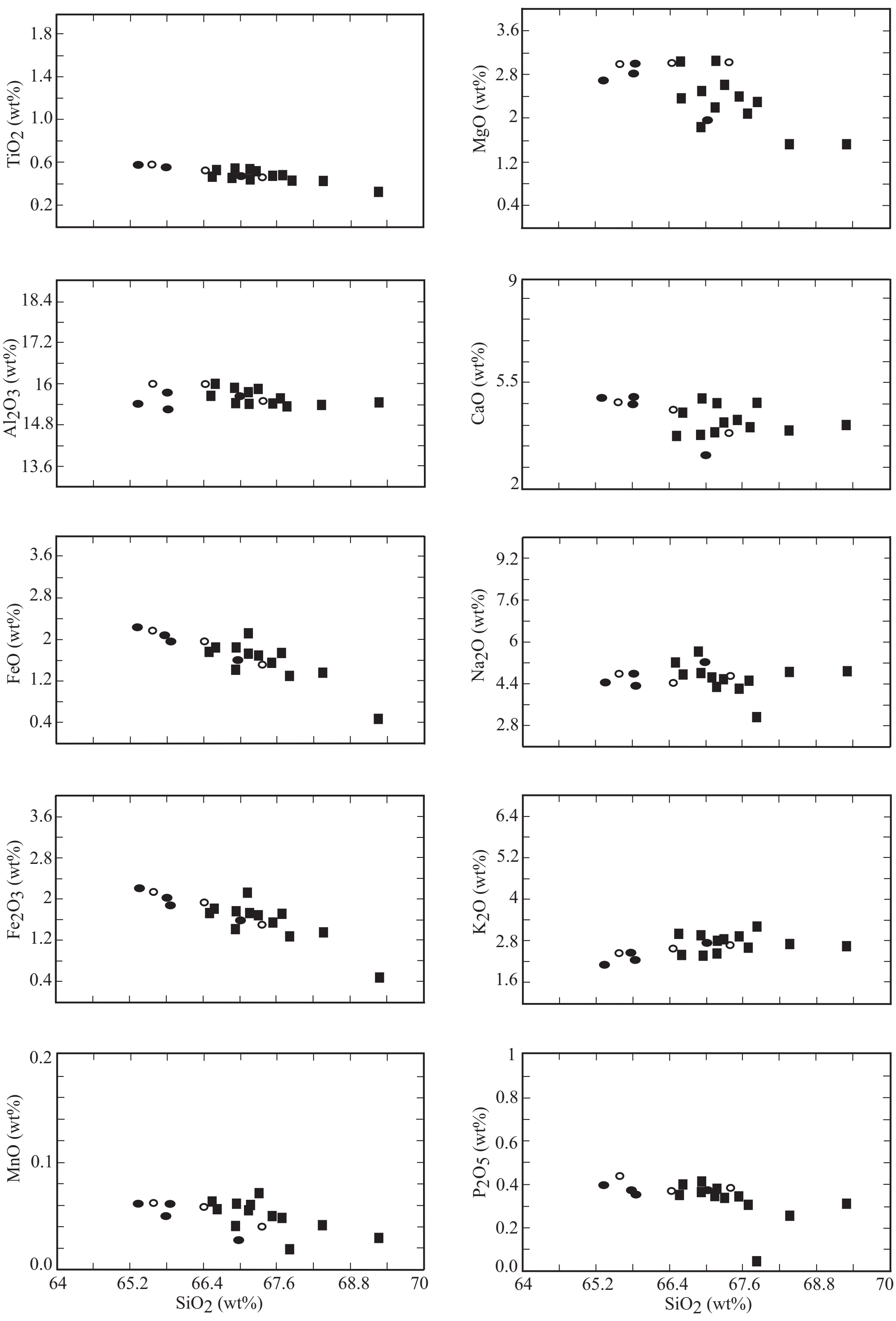

Figure 14. Harker variation diagrams for most major elements of the Sarıhan Granitoid. Filled square– granodiorite, filled circle– Q-monzodiorite; open circle – Q-diorite.

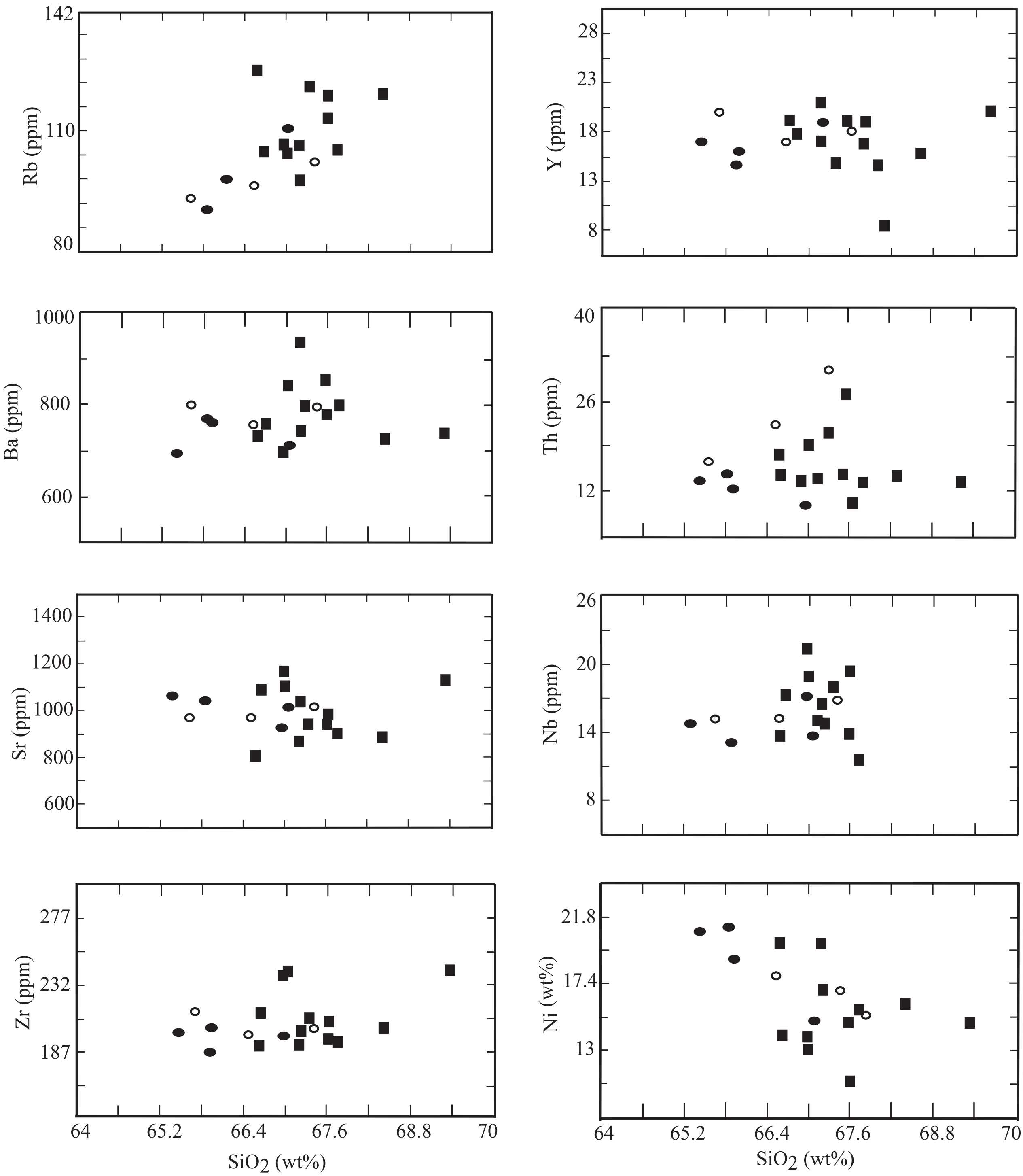

Figure 15. Harker variation diagrams some trace elements of the Sarıhan Granitoid. Filled square– granodiorite, filled circle– Q-monzodiorite; open circle – Q-diorite.

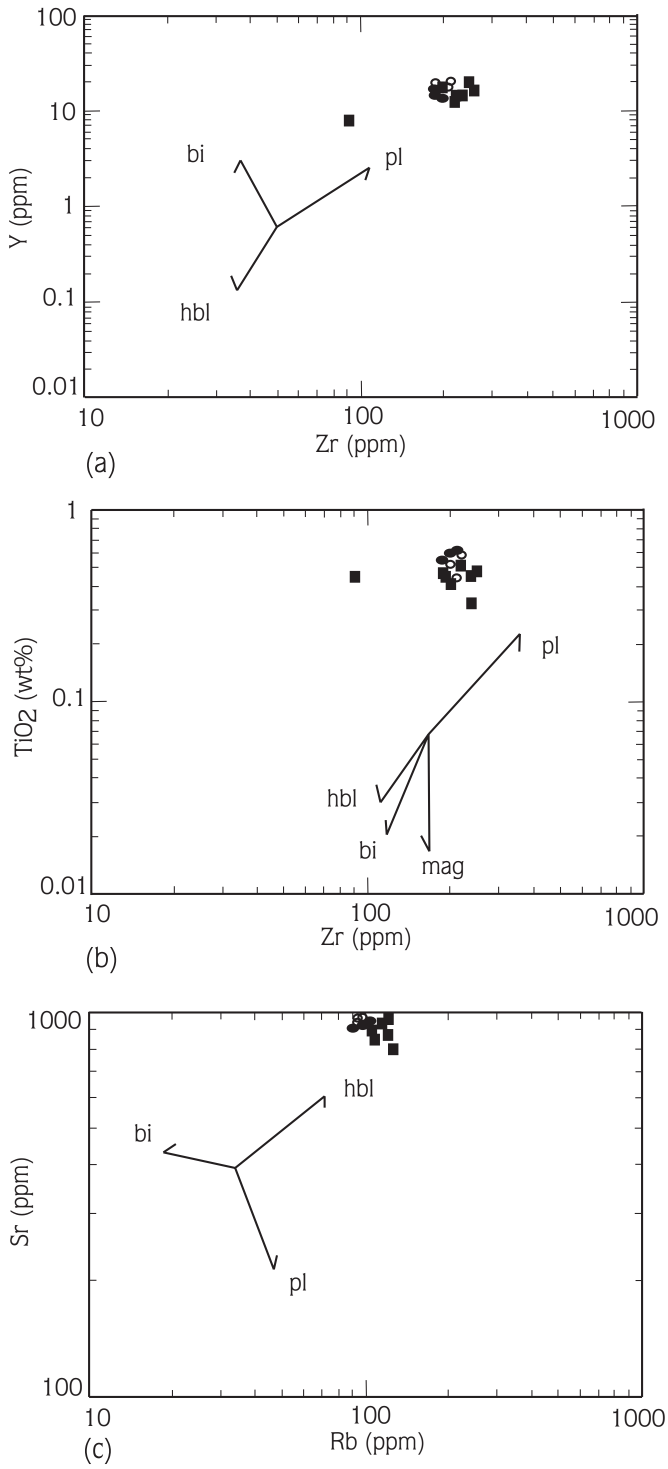

Figure 16. Vectoral diagrams showing fractional crystallisation of minerals. **(a)** Zr-Y vector diagram (after Beckinsale 1979); **(b)** Zr-TiO_2 vector diagram (after Atherton & Sanderson 1985); **(c)** Rb-Sr vector diagram (after Bussel 1988). Filled square– granodiorite, filled circle– Q-monzodiorite; open circle – Q-diorite.

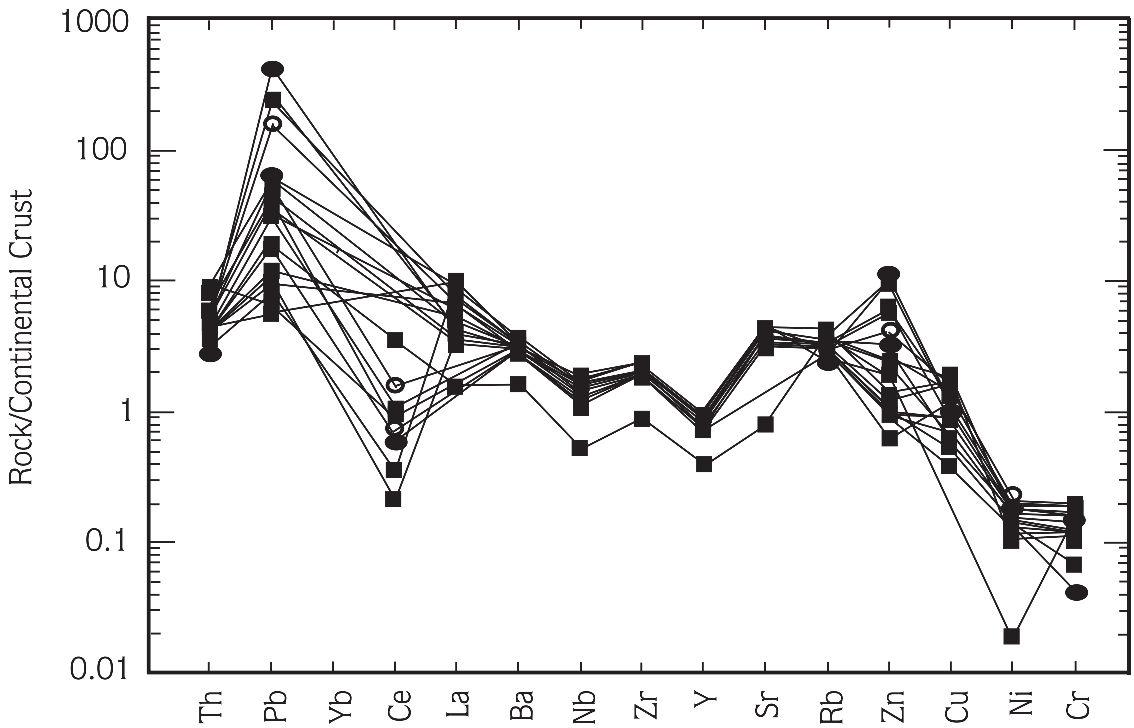

Figure 17. Continental-crust-normalised trace-element diagram (normalised values are from Taylor & Mc Lennan 1985).

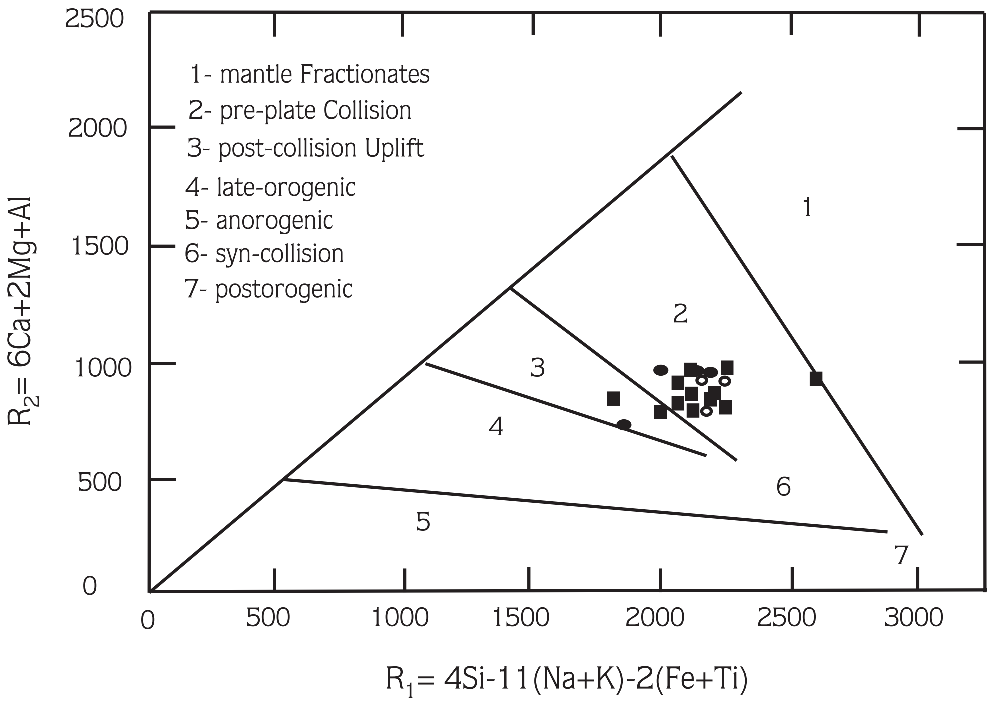

Figure 18. R1-R2 tectonic discrimination diagram of the Sarıhan Granitoid (after Batchelor & Bowden 1985). Filled square– granodiorite, filled circle– Q-monzodiorite; open circle – Q-diorite.

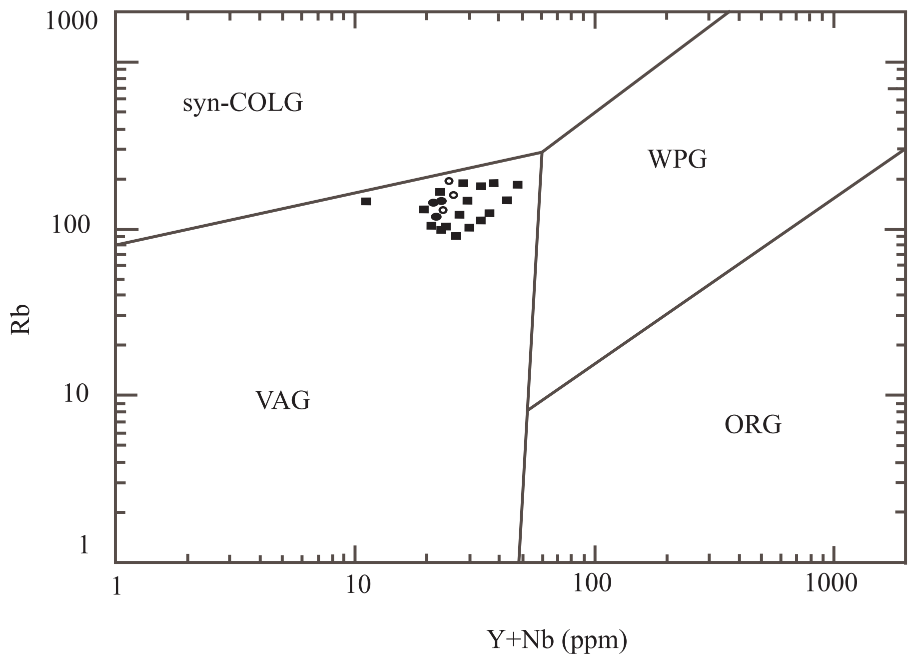

Figure 19. Rb - Y+Nb tectonic diagram (after Pearce *et al*. 1984). Filled square– granodiorite, filled circle– Q-monzodiorite; open circle – Q-diorite.

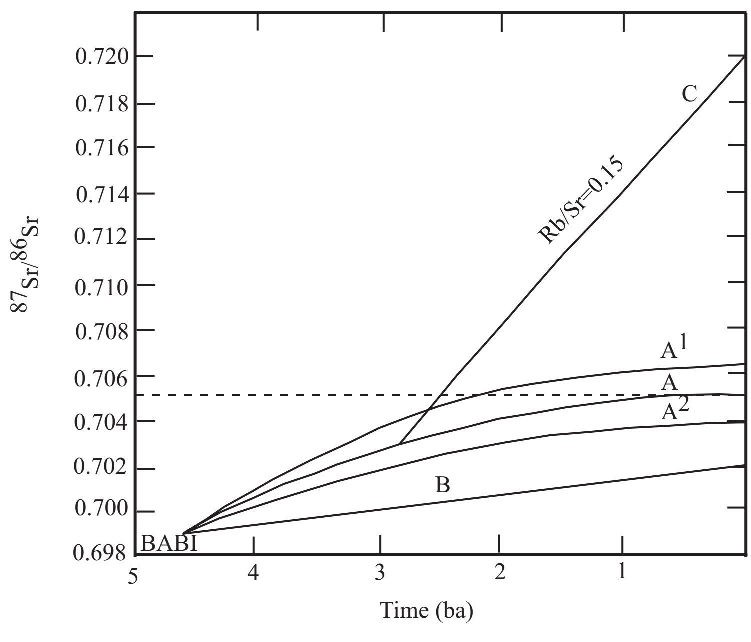

Figure 20. Isotopic evolution of terrestrial Sr. The three curved lines represent hypothetical evolutionary paths of Sr in the mantle under the continents. The curvature of the lines implies a time-dependent decrease in the Rb/Sr ratio of the upper mantle. The straight line (B) connecting BABI to a present value of 0.702 represents strontium evolution in mantle regions depleted in Rb. The diagram also shows a development line (C) for Sr that was withdrawn from mantle about 2.9 billion years ago and resided in a closed system having a Rb/Sr ratio of 0.15 (after Faure 1986).

References

ADAMIA, S.A., LORDKIPANIDZE, M. B. & ZAKARIADZE, G.S. 1977. Evolution of an active continental margin as exemplified by the Alpine history of the Caucasus. *Tectonophysics* **40**, 183–199.

AĞAR, Ü. 1977. *Demirözü (Bayburt) ve Köse (Kelkit) Bölgesinin Jeolojisi* [Geology of Demirözü (Bayburt) ve Köse (Kelkit) Region]. PhD Thesis, Karadeniz Technical University, Trabzon [in Turkish with English abstract].

AKIN, H. 1978. Geologie, Magmatismus und Lager-staettenbidung im ostpontischen Gebirge-Turkei aus der Sicht der Plattentektonik. *Geologische Rundschau* **68**, 253–283.

AKINCI, Ö.T. 1984. The eastern Pontide volcano-sedimentary belt and associated massive sulphide deposits. *In*: DIXON, J.E. & ROBERTSON, A.H.F. (Eds), *The Geological Evolution of the Eastern Mediterranean*. Geological Society Special Publications **17**, 415–428.

ARSLAN, M., TÜYSÜZ, N., KORKMAZ, S. & KURT, H. 1997. Geochemistry and petrogenesis of the eastern Pontide volcanic rocks, northeast Turkey. *Chemie der Erde* **57**, 157–187.

ASLAN, Z. 1998. *Saraycık-Sarıhan Granitoyidleri (Bayburt) ve Çevre Kayaçlarının Petrolojisi, Jeokimyası ve Sarıhan Granitoyidinin Jeokronolojik İncelenmesi* [Petrology-Geochemistry of Saraycık-Sarıhan Granitoids and Their Country Rocks and Geochronology of Sarıhan Granitoid]. PhD Thesis, Karadeniz Technical University, Trabzon [in Turkish with English abstract].

ASLAN, Z. 1999. Sarıhan (Bayburt) Granitoyidinin petrografisi ve mineral kimyası: Doğu Pontid güney zonu, KD Türkiye [Petrography and mineral chemistry of Sarıhan (Bayburt) Granitoid: southern zone of eastern Pontides, NE Turkey]. *Proceedings of the 52nd Geological Congress of Turkey*, 231–238.

ASLAN, Z. & ASLANER, M. 1998b. Evidence of magma mixing and hybrid source on calc-alkaline Sarıhan (Bayburt) Granitoid, NE Turkey. *Mineralogical Magazine* **62A**, 79–80.

ATHERTON, M.P. & SANDERSON, L.M. 1985. The chemical variation and evolution of the super units of the segmented Coastal Batholith. *In:* PITCHER, W.S., ATHERTON, M.P., COBBING, E.J. & BECKINSATE, R.D., (Eds), *Magmatism at a Plate Edge*, 208–227.

BARBARIN, B. 1990. Granitoids: main petrogenetic classifications in relation to origin and tectonic setting. *Geological Journal* **25**, 227–238.

BARBARIN, B. & DIDIER, J. 1992. Genesis and evolution of mafic microgranular enclaves through various types of interaction between coexisting felsic and mafic magmas. *Transactions of the Royal Society of Edinburgh: Earth Sciences* **83**, 145–153.

BATCHELAR, R.A. & BOWDEN, P. 1985. Petrogenetic interpretation of granitoid rock series using multicationic parameters. *Chemical Geology* **48**, 43–55.

BECKINSALE, R.D. 1979. Granite magmatism in the Tin Belt of southeast Asia. *In*: ATHERTON, M.P. & TARNEY, J. (Eds), *Origin of Granite Batholiths: Geochemical Evidence, Shiva, Orpington*, U.K, 34–44.

BEKTAŞ, O., PELİN, S. & KORKMAZ, S. 1984. Doğu Pontid yay gerisi havzasında manto yükselimi ve polijenetik ofiyolit dolgusu [Mantle uplift and polygenetic ophiolites in the eastern Pontide back-arc basin]. *Türkiye Jeoloji Kurumu Ketin Sempozyumu,* 175–188 [in Turkish with English abstract].

BEKTAŞ, O., VAN, A. & BOYNUKALIN, S. 1987. Doğu Pontidlerde Jura volkanizması ve Doğu Pontidler Jeotektoniğindeki yeri [Jurassic volcanism in eastern Pontides and its tectonic significance]. *Türkiye Jeoloji Bülteni* **30**, 9–19 [in Turkish with English abstract].

BOZTUĞ, D. 2001. *Suşehri (Sivas)–Gölköy (Ordu) Arasında KAFZ'nun Kuzey ve Güney Kesimlerindeki Granitoyidlerin ve Çevre Kayaçlarının Petrolojik İncelenmesi* [Petrologic investigation of granitoids and their country rocks exposed in the area between Suşehri (Sivas) and Gölköy (Ordu)]. TÜBİTAK Project Report, Project No. YDABÇAG-9 [unpublished, in Turkish with English abstract].

BOZTUĞ, D., WAGNER, G.A., ERÇİN, A.İ., GÖÇ, D., YEĞİNGİL, Z., İSKENDEROĞLU, A., KURUÇELİK, M.K., KÖMÜR, İ. & GÜNGÖR, Y. 2002. Sphene and zircon fission-track geochronology unravelling subduction- and collision-related magma surges in the composite Kaçkar Batholith, Eastern Black Sea region, Turkey. *1st International Symposium of the Faculty of Mines (İTÜ) on Earth Sciences and Engineering, İstanbul, Turkey, Abstracts,* 121.

BOZTUĞ, D., KUŞÇU, İ., ERÇİN, A.İ., AVCI, N. & ŞAHİN, S.Y. 2003. Mineral deposits associated with the pre-, syn- and post-collisional granitoids of the Neo-Tethyan convergence system between the Eurasian and Anatolian plates in NE and Central Turkey. *In*: ELIOPOULOS, D., *et al.* (Ed), *Mineral Exploration and Sustainable Development*. Millpress, Rotterdam, 1141–1144.

BOZTUĞ, D., JONCKHEERE, R., WAGNER, G.A. & YEĞİNGİL, Z. 2004. Slow Senonian and fast Palaeocene–Early Eocene uplift of the granitoids in the central eastern Pontides, Turkey: apatite fission-track results. *Tectonophysics* **382**, 213–228.

BUSSEL, M.A. 1988. Structure and petrogenesis of a mixed magma ring dyke in the Peruvian Coastal Batholith: eruptions from a zoned magma chamber. *In: The Origin of Granites*. Transactions of the Royal Society of Edinburgh: Earth Sciences, 87–104.

CLARKE, D.B. 1992. *Granitoid Rocks.* Chapman & Hall.

ÇOĞULU, E. 1975. *Gümüşhane ve Rize Granitik Plutonlarının Mukayeseli Petrojeolojik ve Jeokronolojik Etüdü* [Petrogeologic and geochronologic investigation of Gümüşhane and Rize granitic plutons and their comparison]. Dissertation Thesis, İstanbul Technical University [in Turkish with English abstract, unpublished].

DEBON, F. & LE FORT, P. 1982. A chemical-minerogical classification of comman plutonic rocks and associations. *Transactions of the Royal Society of Edinburgh: Earth Sciences* **73**, 135-149.

FAURE, G. 1986. *Principles of Isotope Geology* (2nd Edition). John Wiley & Sons, New York.

Fernandez, A.N. & Barbarin, B. 1991. Relative rheology of coeval mafic and felsic magmas: nature of resulting interaction processes – shape and mineral fabric of mafic microgranular enclaves. *In:* Didier, J. & Barbarin, B. (Eds), *Enclaves and Granite Petrology*. Development in Petrology 13, Elsevier, 263–275.

Förster, H.J., Tischendorf, G. & Trumbull, R.B. 1997. An evalution of Rb vs (Y+Nb) discrimination tectonic setting of silicic igneous rocks. *Lithos* 40, 261–293.

Gedikoğlu, A. 1978. *Harşit Granit Karmaşığı ve Çevre Kayaçlar (Giresun-Doğankent)* [Harşit granit complex and its country rocks (Giresun-Doğankent)]. PhD Thesis, Karadeniz Technical University, Trabzon [in Turkish with English abstract, unpublished].

Güven, İ. H. 1993. *1/250,000-Scale Geological and Metallogenical Map of the Eastern Black Sea Region*. Publications of Mineral Research and Exploration Institute of Turkey (MTA), Trabzon.

Hibbard, M.J. 1991. Textural anatomy of twelve magma mixed granitoid systems. *In*: Didier, J. & Barbarin, B. (Eds), *Enclaves and Granite Petrology*. Development in Petrology 13, Elsevier, 431–444.

Hammarstrom, J.M. & Zen, E.A. 1986. Aluminum in hornblende: an empirical igneous geobarometer. *American Mineralogist* 71, 1297–1313.

Hollister, L.S., Grisson, G.C., Peters, E.K., Stowell, H.H. & Sisson, V.B. 1987. Confirmation of the empirical calibration of Al in hornblende with pressure of solidification of calc-alkaline plutons. *American Mineralogist* 72, 231–239.

Irvine, T.N. & Baragar, W.R.A. 1971. A guide to the chemical classification of the common volcanic rocks. *Canadian Journal of Earth Sciences* 8, 523–543.

Karsli, O., Aydin, F. & Sadiklar M.B. 2004. Magma interaction recorded in plagioclase zoning in granitoid systems, Zigana Granitoid, Eastern Pontides, Turkey. *Turkish Journal of Earth Sciences* 13, 287–306.

Keskin, İ., Korkmaz, S., Gedik, İ., Ateş, M., Gök, L., Küçümen, Ö. & Erkal, T. 1989. *Bayburt Dolayının Jeolojisi* [Geology of Bayburt region]. Mineral Research and Exploration Institute of Turkey (MTA) Project Report [unpublished, in Turkish].

Ketin, İ. 1966. Anadolu'nun tektonik birlikleri [Tectonic units of Anatolia]. *MTA Dergisi* 66, 20–34.

Lameyre, J. & Bonin, B. 1991. Granites in the main plutonic series. *In:* Didier, J. & Barbarin, B. (Eds), *Enclaves and Granite Petrology.* Development in Petrology 13, Elsevier, 3–17.

Leake, B.E. 1978. Nomenclature of amphiboles. *American Mineralogist* 63, 1025–1032.

Leake, B.E. & Said, Y.A. 1994. Hornblende barometry of the Galway Batholith, Ireland; an empirical test. *Mineralogy & Petrology* 51, 243–250.

Maniar, P.D. & Piccoli, P.M. 1989. Tectonic discrimination of granitoids. *Geological Society of America Bulletin* 101, 635–643.

Moore, W.J., Mckee, E.H. & Akinci, Ö. 1980. Chemistry and chronology of plutonic rocks in the Pontid mountains, northern Turkey. *Symposium*: *European Copper Deposits, Belgrade*, 209–216.

Okay, A.İ. & Şahintürk, Ö. 1997. Geology of the eastern Pontides. *In*: Robinson, A.G. (Ed), *Regional and Petroleum Geology of the Black Sea and Surrounding Region*. AAPG Memoir 68, 291–311.

Pearce, J.A., Harris, N.B.W. & Tindle, A.G. 1984. Trace element discrimination diagrams for the tectonic interpretation of granitic rocks. *Journal of Petrology* 25, 956–983.

Pitcher, W.S. 1993. *The Nature and Origin of Granite*. Chapman & Hall.

Robinson, A.G., Banks, C.J., Rutherford, M.M. & Hirst, J.P.P. 1995. Stratigraphic and structural development of the eastern Pontides, Turkey. *Journal of Geological Society, London* 152, 861–872.

Shelley, D. 1993. *Igneous and Metamorphic Rocks Under the Microscope*. Chapman and Hall, London.

Stamatelopoulou-Seymour, K., Vlassopoulos, D., Pearce, T.H. & Rice, C. 1990. The record of magma chamber processes in plagioclase phenocrysts at Thera Volcano, Aegean volcanic arc, Greece. *Contributions to Mineralogy and Petrology* 104, 73–84.

Şen, C. & Kaygusuz, A. 1998. Doğu Pontid adayayı granitoyidlerin karşılaştırılmalı petrografik ve kimyasal özellikleri, KD Türkiye [Petrographic and chemical characteristics and comparison of eastern Pontide granitoids, NE Turkey]. *Fırat Üniversitesi Jeoloji Mühendisliği Eğitiminin 20. Yılı Sempozyumu Bildiri Özleri Kitabı, Elazığ,* 12–13.

Şengör, A.M. & Yilmaz, Y. 1981. Tethyan evolution of Turkey: a plate tectonic approach. *Tectonophysics* 75, 181–241.

Taner, M.F. 1977. *Etuda géologique et pétrographique de la région de Güneyce-İkizdere, située au sud de Rize (Pontides orientales, Turquie)*. PhD Thesis, Universite de Geneve.

Tanyolu, E. 1988. Pulur Masifi (Bayburt) Doğu Kesiminin Jeolojisi [Geology of eastern part of Pulur Massif]. *MTA Dergisi* 108, 1–18.

Taylor, Y & Mc Lennon, S.M. 1985. *The Continental Crust: Its Composition and Evolution*. Blackwell, Oxford.

Topuz, G. 2000. *Zur Petrologie der metamorphen Gesteine des Pulur Massivs (Östliche Pontiden, Türkei)*. PhD Thesis, Ruprecht Karls Universitaet, Heidelberg, Germany.

Van, A. 1990. *Pontid Kuşağında Artvin Bölgesinin Jeokimyası, Petrojenezi ve Masif Sülfit Mineralizasyonları* [Geochemistry, petrogenesis and massive sulphide mineralizations of Artvin region, eastern Pontides]. PhD Thesis, Karadeniz Technical University, Trabzon [in Turkish with English abstract, unpublished].

Vernon, R.H. 1984. Microgranitoid enclaves in granites: globules of hybrid magma quenched in a plutonic environment. *Nature* 309, 438–439.

Vernon, R.H. 1991. Interpretation of microstructures of microgranitoid enclaves. *In*: Didier, J. & Barbarin, B. (Eds), *Enclaves and Granite Petrology*. Development in Petrology 13, Elsevier, 277–292.

YILMAZ, Y. 1972. *Petrology and Structure of the Gümüşhane Granite and Surrounding Rocks, North-eastern Anatolia.* PhD Thesis, University of London [unpublished].

YILMAZ, S. & BOZTUĞ, D. 1994. Granitoyid petrojenezinde magma mingling/mixing kavramı [Magma mingling/mixing processes in granitoid petrogenesis]. *Jeoloji Mühendisliği* 44/45, 1–20 [in Turkish with English abstract].

YILMAZ, S. & BOZTUĞ, D. 1996. Space and time relations of three plutonic phases in the Eastern Pontides, Turkey. *International Geology Review* 38, 935–956.

YILMAZ, Y., TÜYSÜZ, O., YIĞITBAŞ, E., GENÇ, Ş.C. & ŞENGÖR, A.M.C. 1997. Geology and tectonic evolution of the Pontides. *In*: ROBINSON, A.G. (Ed), *Regional and Petroleum Geology of the Black Sea and Surrounding Region.* AAPG Memoir 68, 183–226.

Received 09 August 2003; revised typescript accepted 25 March 2005